

Structural relaxation in the glass transition region of water

Nicolas Giovambattista,^{1,2} C. Austen Angell,³ Francesco Sciortino,⁴ and H. Eugene Stanley¹

¹*Center for Polymer Studies and Department of Physics, Boston University, Boston, Massachusetts 02215 USA*

²*Department of Chemical Engineering, Princeton University, Princeton, New Jersey 08544-5263 USA*

³*Department of Chemistry and Biochemistry Arizona State University, Tempe, Arizona 85287 USA*

⁴*Dipartimento di Fisica, Istituto Nazionale per la Fisica della Materia and INFM-CRS-SOFT: Complex Dynamics in Structured Systems, Università di Roma La Sapienza, Piazzale Aldo Moro 2, I-00185 Roma, Italy*

(Received 29 November 2004; published 19 July 2005)

We perform molecular dynamics (MD) simulations using the extended simple-point-charge (SPC/E) model for water to study the structural relaxation through the glass transition region. We follow the same standard protocol used in differential scanning calorimetry experiments. Specifically, we cool liquid configurations at different cooling rates to produce a glass, and then we heat the glass back to the liquid state. We also study aging effects in the glass before heating. We find that MD simulations can reproduce the phenomenology observed in experiments. We review the Tool-Narayanaswamy-Moynihan (TNM) phenomenological approach, introduced to describe the behavior of the specific heat upon heating glass to the liquid phase. The TNM approach requires, as an ansatz, an expression for the temperature dependence of the relaxation time. We compare the simulation results with the prediction of the TNM approach supplemented with two well-known expressions for the relaxation time: the Narayanaswamy-Moynihan (NM) and the Adam-Gibbs-Scherer (AGS) expressions. We find that, in the case of slow cooling rates, our simulations are well represented by the TNM approach, but only if the AGS expression is adopted. We also find that the TNM approach fails in the case of fast cooling rates for both NM and AGS expressions. Several attempts to provide more freedom to the fitting procedure by allowing the fitting parameters to depend on temperature, cooling, and/or heating rates do not improve the agreement between the simulation data and the TNM predictions.

DOI: [10.1103/PhysRevE.72.011203](https://doi.org/10.1103/PhysRevE.72.011203)

PACS number(s): 82.40.Bj, 05.45.Ac

I. INTRODUCTION

Liquids crystallize upon cooling. However, in some materials, the liquid can be cooled to a metastable state down to a temperature T so that the characteristic time becomes much larger than typical slow experimental time scales (100 s). In these cases, the system is arrested in a disordered configuration called the glass state [1–3]. The formation of the glass state prevents the crystallization of the system. Conventionally, the glass transition temperature T_g is identified as the T at which the characteristic time scales are of the order of 100 s.

In the glass state, the system is trapped in an out-of-equilibrium configuration. Glasses are thus characterized by extremely slow phenomena, expressing the attempt of the system to reach equilibrium through the rearrangement of the molecular structure. This relaxation is called “structural relaxation” [4,5]. Structural relaxation takes place when the glass is cooled, heated, or kept at a finite temperature below T_g [6–9]. The isothermal evolution of the system driven by structural relaxation is also known as “aging” or “annealing.”

Differential scanning calorimetry (DSC) [5] is a widely used technique for studying structural relaxation. In these experiments, a liquid is cooled below T_g and the specific heat is measured upon heating the glass back to the liquid phase. Typical cooling and heating rates are found in the range of 1–10⁵ K/s. The behavior of the specific heat upon heating changes dramatically with the glass history. For example, depending on the cooling and/or heating rate used in the experiment, an exothermic or endothermic peak in the specific heat preceding the glass transition can be observed

[10–12]. The effects on the DSC measurements of the cooling and heating rates have been studied in many substances—e.g., 5-phenyl-4-ether [10], poly(vinyl chloride) [11], poly(vinyl Acetate) [13], polystyrene [14], B₂O₃ [15], inorganic glasses [16], and, more recently, in computer simulations [17]. Furthermore, Hodge and Berens have shown that aging in the glass state [6,7] drastically changes the behavior of the specific heat upon heating. The phenomenology associated with these experiments is very rich and well documented (see, e.g., Refs. [4,5]).

Few analytical approaches [18] have been proposed to describe structural relaxation through the glass transition region. In particular, the phenomenological Tool-Narayanaswamy-Moynihan (TNM) approach [10,19,20] has been widely used to interpret experimental data. This approach depends on a few fitting parameters obtained from experiments and requires an ansatz for the T dependence of the relaxation time of the system. The most common expressions for the relaxation time are the Narayanaswamy-Moynihan (NM) [10,20] and the Adam-Gibbs-Scherer (AGS) expressions [21,22]. The predictions of the TNM approach have been tested in many experiments for different cooling and heating rates (see e.g., Refs. [5,10,23,24]). A successful extension of the TNM approach has been proposed by Hodge and co-workers to predict the effects of aging in polymer samples [7,14,25]. In this work, we extend the application of the TNM approach to describe results from molecular dynamics (MD) simulations of water across T_g with different thermal histories.

This work is an extension and continuation of a preliminary report [17] and is organized as follows. In Sec. II we

provide simulation details. In Sec. III we review the TNM approach and the numerical algorithm implemented to describe our simulation results. In Sec. IV we present our results. First, we show that the phenomenology associated with the glass transition can be reproduced in MD simulations. Then, we extensively test the TNM approach using both the NM and the AGS expressions. We study different cooling and heating thermal histories, as well as thermal histories involving aging. We discuss the limitations of the TNM approach in Sec. V.

II. SIMULATIONS

We perform MD simulations for a system of $N=216$ molecules interacting with the extended simple-point-charge (SPC/E) potential [26], with periodic boundary conditions. Interactions are cut at a distance of $r=2.5\sigma$ (σ is defined in the SPC/E potential) and reaction field corrections are added to account for the long-range interactions. Quantities are averaged over 32 independent trajectories obtained at a fixed density $\rho=1$ g/cm³.

We perform three types of MD calculations: (i) cooling runs at constant rate, starting from equilibrium (liquid) configurations at $T=300$ K, (ii) heating runs at constant rate (from glass configurations at 5 K), and (iii) aging runs at constant temperature (at 100 and 180 K, where a significant aging dynamics is observed).

We study cooling rates ranging from $q_c=-10^5$ K/ns to $q_c=-30$ K/ns and a single heating rate of $q_h=+30$ K/ns. An averaged cooling-heating run with our slowest rate ± 30 K/ns requires a simulation lasting 320 ns, close to the maximum possible by our method. On the other hand, cooling runs at a rate of $q_c=-10^5$ K/ns are the fastest we can simulate in order to obtain reliable data. At every simulation time step the thermostat temperature is increased by $\delta T=q\delta t$, where $\delta t=1$ fs is the simulation time step and q is the cooling-heating rate. The temperature is increased by rescaling the velocities of the molecules. We control the temperature using the Berendsen thermostat [27] with a relaxation constant of 0.1 ps.

III. TOOL-NARAYANASWAMY-MOYNIHAN APPROACH

A. The approach

More than 30 years ago, Narayanaswamy [20] proposed a phenomenological approach to describe the structural relaxation kinetics (i.e., the gradual approach of the properties of the system to their equilibrium values) under any thermal history defined by the time evolution of T . His approach builds on Tool's work [19], who introduced the basic concept of the fictive temperature T_f . Narayanaswamy's approach was adapted and extensively tested by Moynihan *et al.* [10]. In the following we review the resulting TNM approach following the work of Moynihan *et al.* [10] (a more detailed description can be found in Refs. [4,5,7,10]).

To begin, we introduce the concept of fictive temperature $T_f(T)$ in the context of constant volume cooling and heating runs. To do this, we first discuss the T dependence of the total energy of the system $e(T)$ upon cooling and heating the

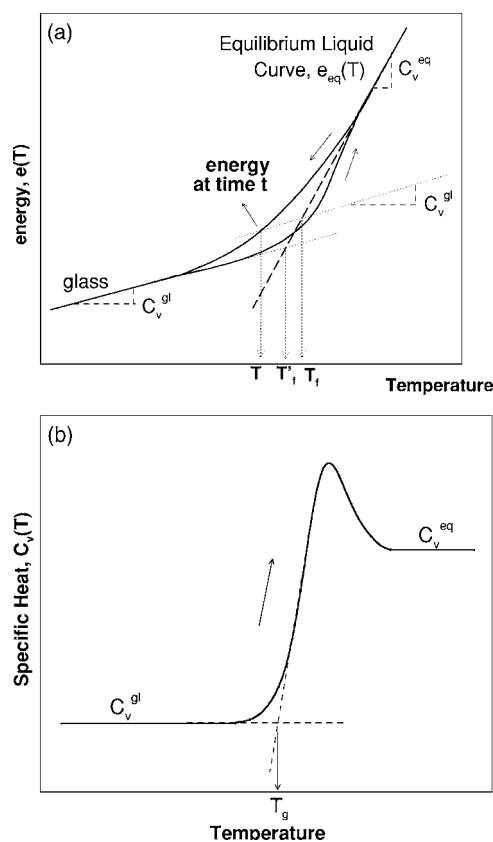


FIG. 1. (a) Scheme showing the typical temperature dependence of a macroscopic property, in this case the total energy $e(T)$, when a liquid is slowly cooled to the glassy state and heated back to the liquid phase (at a rate comparable to the cooling rate). Upon cooling, $e(T)$ departs from the equilibrium liquid curve $e_{eq}(T)$ (long-dashed line) at high T . Instead, on reheating, the $e(T)$ curve overshoots the $e_{eq}(T)$ curve. The fictive temperature of the system $T_f(T)$, when the bath temperature is T , can be obtained by the construction shown in the figure [corresponding to the definition given in Eq. (1)]. The value of $T_f(T)$ for $T \rightarrow 0$ —i.e., when the system reaches the glassy state—is denoted by T_f^g . (b) Typical behavior of the specific heat $C_v(T)$ upon heating a slow-cooled glass, calculated by differentiating $e(T)$ in (a). The glass transition temperature T_g , which can be defined graphically by intersecting the two dashed lines in the figure, is followed by a peak in $C_v(T)$. C_v^{gl} and C_v^{eq} denotes the specific heat when the system is in the glassy state and the equilibrium liquid phase, respectively. These two quantities may depend on temperature (in the case of experiments at constant P , the specific heat in the glassy state can have a strong T dependence and goes to zero at $T=0$).

system across T_g [see Fig. 1(a)]. A cooling-heating run with a rate $q=\delta T/\delta t$ can be thought of as a series of differential temperature steps ΔT , each of which is followed by an isothermal hold of $\Delta t=\Delta T/q$. During the initial stage of the cooling shown in Fig. 1(a), the T is high enough so that $\Delta t > \tau(T)$, where $\tau(T)$ is the structural relaxation time of the system. Under this condition, the system has time to relax to equilibrium before T changes considerably. Consequently, $e(T)$ coincides with the energy of the system in equilibrium, $e_{eq}(T)$, as shown in Fig. 1(a). At lower T , $\Delta t < \tau(T)$ and the system is unable to reach equilibrium during the time Δt .

Therefore, upon cooling at low T , $e(T)$ deviates from $e_{\text{eq}}(T)$. On reheating the glass back to the liquid phase, $e(T)$ evolves along a different path than the one followed upon cooling and, for similar cooling and heating rates, $e(T)$ “overshoots” the equilibrium curve $e_{\text{eq}}(T)$ [see Fig. 1(a)]. Such an overshoot is responsible for the peak in the specific heat, $C_V(T)$, characterizing the glass transition upon heating. Figure 1(b) shows the corresponding behavior of $C_V(T)$ upon heating the glass. The specific heat in the glass state, $C_V^{\text{gl}}(T)$, is usually weakly T dependent. At high T , $C_V(T)$ approaches the equilibrium liquid specific heat $C_V^{\text{eq}}(T)$.

Figure 1(a) shows the construction used to define $T_f(T)$ [10]. This construction corresponds to the following implicit definition of $T_f(T)$ [28]:

$$e_{\text{eq}}(T_f) = e(T) + \int_T^{T_f} C_V^{\text{gl}}(T) dT. \quad (1)$$

Here $e_{\text{eq}}(T_f)$ is the energy of the system in the equilibrium liquid phase at temperature T_f , $C_V^{\text{gl}}(T)$ denotes the specific heat of the system in the glass state at T or its extrapolation at temperature T , and T_f is the temperature at which the equilibrium liquid would have the same energy as the glass found at T , once it is heated up to T_f . Note that Eq. (1) accounts for a possible T dependence of $C_V^{\text{gl}}(T)$. An equivalent definition for $T_f(T)$ to that given in Eq. (1) can be obtained by differentiating both sides of Eq. (1) with respect to T . Thus, we find that

$$\frac{dT_f}{dT} = \frac{C_V(T) - C_V^{\text{gl}}(T)}{C_V^{\text{eq}}(T_f) - C_V^{\text{gl}}(T_f)}, \quad (2)$$

where $C_V(T) \equiv (\partial e(T)/\partial T)_v$ is the out-of-equilibrium specific heat and $C_V^{\text{eq}}(T_f)$ is the specific heat in the equilibrium liquid phase at T_f (or its extrapolation at T_f).

Equations (1) and (2) relate an observable, $e_{\text{eq}}(T)$ or $C_V(T)$, with $T_f(T)$. The physical meaning of T_f is that $T_f(T) - T$ measures (in T units) how far the system is from equilibrium when the bath temperature is T . The TNM approach allows the prediction of the functional dependence of $T_f(T)$ for any arbitrary thermal history $T(t)$; it also predicts the behavior of $e(T)$ and $C_V(T)$ by using Eqs. (1) and (2).

Next we review the expression for $T_f(T)$ proposed by the TNM approach. There are three different cases depending on the complexity of $T(t)$.

(i) *The bath temperature $T(t)$ is suddenly changed at $t = t_0$ by a small amount ΔT from an equilibrium state with a temperature T_0 .* In this case, $T_f(t)$ can always be expressed as

$$T_f(t) \equiv T_0 + \Delta T [1 - \phi(t_0, t)], \quad (3)$$

where $\phi(t_0, t)$ is the “response function” of the system. For a system with an instantaneous response, $\phi(t_0, t) = 1 - \theta(t - t_0)$, where $\theta(x)$ is the Heaviside function [$\theta(x) = 1$ for $x > 0$ and $\theta(x) = 0$ for $x \leq 0$]. In the case of structural relaxation, $\phi(t_0, t)$ can be approximated by a Kohlrausch-Williams-Watts (KWW) or stretched exponential function [29]

$$\phi(t_0, t) = \begin{cases} \exp\left[-\left(\frac{t-t_0}{\tau}\right)^\beta\right] & \text{if } t > t_0, \\ 1 & \text{otherwise.} \end{cases} \quad (4)$$

Here, $0 < \beta \leq 1$ is the stretching exponent and τ is the relaxation time. It is found that $\beta < 1$ in supercooled liquids and glasses, implying that the relaxation is nonexponential.

(ii) *The bath temperature $T(t)$ is suddenly changed at $t = t_0$ by a large amount ΔT from an equilibrium state with a temperature T_0 .* Gardon and Narayanaswamy [20] showed that when ΔT is not small, the relaxation is not only nonexponential, but also nonlinear; i.e., ϕ in Eq. (3) also depends on $T_f(T)$. Gardon and Narayanaswamy [20] proposed that for large ΔT the response function can be expressed as

$$\phi(t_0, t) = \begin{cases} \exp\left[-\left(\int_{t_0}^t \frac{dt'}{\tau(T(t'), T_f(t'))}\right)^\beta\right] & \text{if } t > t_0, \\ 1 & \text{otherwise,} \end{cases} \quad (5)$$

and

$$\tau(T(t'), T_f(t')) = A \exp\left[\frac{x\Delta h^*}{RT(t')} + \frac{(1-x)\Delta h^*}{RT_f(t')}\right]. \quad (6)$$

Here $0 \leq x \leq 1$, Δh^* and A are constants, and R is the ideal gas constant. We refer to Eq. (6) as the Narayanaswamy-Moynihan expression. We note that for $\Delta T \rightarrow 0$, one expects that $\tau(T, T_f) \approx \tau(T_0) = A \exp(\Delta h^*/RT_0) \approx \text{const}$. Thus, Eq. (5) reduces to Eq. (4).

(iii) *The bath temperature $T(t)$ changes arbitrarily with time.* In this case, the evolution of T_f under an arbitrary perturbation $T(t)$ cannot be described by a simple expression such as Eq. (3). Instead, the TNM approach proposes that

$$T_f(t) = T_0 + \int_{T_0}^T dT' [1 - \phi(t', t)], \quad (7)$$

where ϕ is given by Eq. (5) and t' inside the integral is the time at which the bath temperature is T' . In other words, Eq. (7) implies that the evolution of T_f with time is due to the *linear superposition* of infinitesimal perturbations dT' that occur at times t' [each one producing the same response of the form given by Eqs. (3) and (5)]. When the time dependence of T is characterized by a finite cooling-heating rate (i.e., no isothermal aging), then one can express it as $dt = dT/q(t)$. Therefore, introducing Eq. (5) into Eq. (7) we obtain the final TNM expression

$$T_f(t) = T_0 + \int_{T_0}^T dT' \left\{ 1 - \exp\left[-\left(\int_{T'}^T \frac{dT''}{q(T'')\tau(T'', T_f)}\right)^\beta\right] \right\}. \quad (8)$$

The TNM approach with the relaxation time provided by Eq. (6) has been successfully applied to many systems [10,11,13–15]. However, due to the lack of a firm theoretical justification for Eq. (6), other expressions for $\tau(T, T_f)$ have been proposed. Scherer [22] proposed an expression for $\tau(T, T_f)$ based on the Adam-Gibbs [21] expression, where he

assumed that the configurational entropy S_c is a function of T_f —i.e.,

$$\tau(T(t'), T_f) = A \exp \left[\frac{E_A}{S_c(T_f) T(t')} \right], \quad (9)$$

with

$$S_c(T) = \int_{T_K}^T \frac{\Delta C}{T} dT. \quad (10)$$

Here T_K is the Kauzmann temperature [2] and ΔC is the difference between the specific heat capacities of the liquid and glass. We refer to Eq. (9) as the Adam-Gibbs-Scherer expression.

We note that the TNM approach with the NM expression requires four fitting parameters ($A, x, \Delta h^*$, and β). Similarly, the TNM approach complemented by the AGS expression requires four parameters (A, E_A, T_K , and β). However, in computer simulations $S_c(T)$ and therefore T_K can be calculated independently [30–32], reducing the number of fitting parameters when using the AGS expression from four to three (A, E_A , and β).

B. Implementation of the TNM approach and its fitting parameters

Next, we discuss how to apply the TNM approach to describe structural relaxation and how to obtain the fitting parameters from MD simulations. This procedure follows the one employed by Hodge and Berens in their analysis of experimental data [7]. The fitting parameters in the TNM approach are system dependent and estimated from preliminary experiments and simulations. To calculate these parameters it is necessary to discretize the time variable in the equations described above—in particular, Eqs. (1), (6), (8), and (9). Equation (8) can be rewritten as

$$T_{f,n} = T_o + \sum_{j=1}^n \Delta T_j \left\{ 1 - \exp \left[- \left(\sum_{k=j}^n \frac{\Delta T_k}{q_k \tau_k} \right)^\beta \right] \right\}, \quad (11)$$

where $T(t) \rightarrow T_n$ and n is the number of sampling points. The NM and AGS expressions for τ in Eqs. (6) and (9) can be rewritten as

$$\tau_k = A \exp \left[\frac{x \Delta h^*}{R T_k} + \frac{(1-x) \Delta h^*}{R T_{f,k-1}} \right], \quad (12)$$

$$\tau_k = A \exp \left[\frac{E_A}{S_c(T_{f,k-1}) T_k} \right]. \quad (13)$$

To discretize Eq. (1), we first approximate $C_V^{\text{gl}}(T) \approx a_0 T + b_0$ [22,33]. Therefore, Eq. (1) can be rewritten as

$$e(T_n) - \frac{a_0}{2} T^2 - b_0 T = e_{\text{eq}}(T_{f,n}) - \frac{a_0}{2} T_{f,n}^2 - b_0 T_{f,n}. \quad (14)$$

We use the following procedure to find the fitting parameters.

(i) Evaluate $e(T_n)$ for all n from MD simulations for a given thermal history $T(t)$.

(ii) Choose the parameters ($A, x, \Delta h^*$, and β) when using

the NM expression for τ_k , or (A, E_A , and β) when using the AGS expression. In the last case, we do not need to use T_K as a fourth fitting parameter because $S_c(T)$ for the SPC/E model has been previously calculated [31].

(iii) Predict the values of $T_{f,n}$ for all n using Eq. (11) and Eq. (12) and (13).

(iv) Use the $T_{f,n}$ values calculated in point (iii) together with the known T dependence of the equilibrium energy to evaluate the “error function” [34,35]

$$\psi = \sum_n \{ [e(T_n) - a_0/2T^2 - b_0T] - [e_{\text{eq}}(T_{f,n}) - a_0/2T_{f,n}^2 - b_0T_{f,n}] \}^2 \Delta T_n \quad (15)$$

based on Eq. (14).

(v) Iterate steps (ii)–(iv) until ψ reaches the minimum in the fitting parameters space.

The fitting parameters in the TNM approach are independent of the thermal history $T(t)$. In other words, for any $T(t)$, Eqs. (11) [together with Eqs. (12) and (13)] and (14) should predict the measured [or simulated] $C_V(T)$ [or equivalently $e(T)$] with the same set of fitting parameters. Therefore, to perform a proper test of the TNM approach, we will calculate the fitting parameters for different thermal histories. From the scatter in the set of parameters, an estimate of the performance of the TNM approach can be obtained.

IV. RESULTS

A. Phenomenology of the glass transition from MD simulations

In this section we show how computer simulations reproduce the features characteristic of the DSC experimental results. MD simulations can thus be used to study the glass transition even if the simulation time scales are $\approx 10^9$ times smaller than those typically studied experimentally.

Differential scanning calorimetry is a standard experimental technique for studying the glass transition. In these experiments, the equilibrium liquid is cooled down to the glass state with a small cooling rate $q_c \equiv dT/dt$ (typically $|q_c| \approx 1-100$ K/s [29]). The glass is then slowly heated back up to the liquid phase with a heating rate q_h . These experiments are performed at a constant pressure and the isobaric specific heat $C_p(T)$ is measured upon heating. The typical behavior of $C_p(T)$ for $q_h \approx -q_c$ is similar to the schematic behavior of $C_V(T)$ indicated in Fig. 1(b). We note that the specific heat in the glass and in the equilibrium liquid phase may be T dependent.

MD simulations reproduce the glass transition phenomenology discussed above. To show this, we quench the equilibrium liquid configurations at a constant volume from $T = 300$ K down to $T \approx 0$ at a constant cooling rate of $q_c = -30$ K/ns and then heat the glass back to the liquid phase at a constant heating rate of $q_h = -q_c = +30$ K/ns. The $C_V(T)$ for the $(-30/+30)$ trajectory (i.e., $q_c = -30$ K/ns and $q_h = 30$ K/ns) is shown in Fig. 2(a) and is similar to the scheme shown in Fig. 1(b). However, $C_V(T)$ in Fig. 2(a) shows a strong T dependence at high T . Specifically, we find that

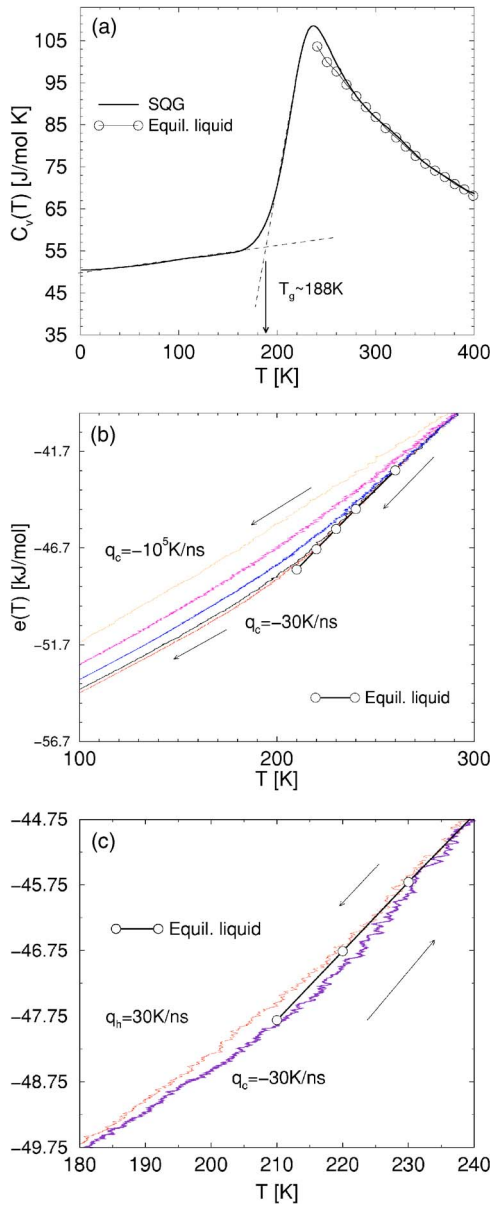


FIG. 2. (Color online) (a) Specific heat $C_V(T)$ obtained upon heating the slow-quenched glass SQG (the glass obtained with a cooling rate $q_c = -30$ K/ns) at a rate of $q_h = 30$ K/ns. Comparison with Fig. 1(b) shows a weak T dependence of $C_V^{eq}(T)$ [33] but a strong T dependence of $C_V(T)$. The glass transition temperature T_g is also indicated. (b) Energy $e(T)$ obtained upon cooling liquid configurations at cooling rates $q_c = -30, -10^2, -10^3, -10^4$, and -10^5 K/ns. The larger the $|q_c|$, the higher the $e(T)$ is at the glass state and the higher the T at which $e(T)$ departs from the equilibrium values. (c) $e(T)$ upon cooling and heating in the $(-30/+30)$ run. In agreement with experiments [see also Fig. 1(a)], the system reaches equilibrium upon heating at a T higher than the T at which it departs from equilibrium upon cooling.

$C_V^{eq}(T)$ decreases as T increases. We note that a decrease of $C_V^{eq}(T)$ with T also seems to occur in real water above 40°C [36]. We also note that Fig. 2(a) shows that $T_g \approx 188$ K for the $(q_c/q_h) = (-30/+30)$ temperature profile.

Figure 2(b) shows $e(T)$ upon cooling equilibrium liquid configurations to the glass state at different q_c . Correspond-

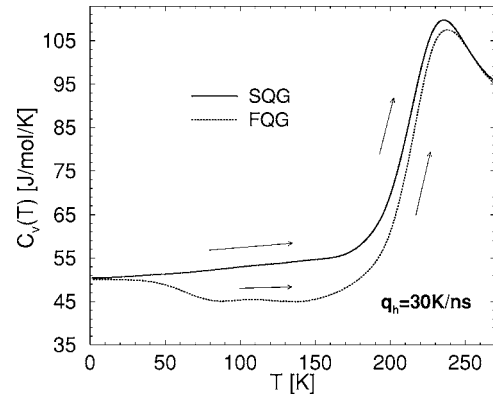


FIG. 3. Specific heat $C_V(T)$ upon heating different glasses. The slow-quenched glass (SQG) is generated by cooling liquid configurations at $q_c = -30$ K/ns while the fast-quenched glass (FQG) is generated with $q_c = -10^4$ K/ns. A valley in $C_V(T)$ develops upon heating the FQG at $q_h = 30$ K/ns, in agreement with experimental results.

ing with experiments, we find that the higher the $|q_c|$, the higher the T at which $e(T)$ deviates from the equilibrium liquid energy $e_{eq}(T)$ (indicated by circle symbols in the figure) and the final value of $e(T)$ in the glass state. Figure 2(c) shows $e(T)$ when the system is cooled at $q_c = -30$ K/ns and the glass is heated back to the liquid phase at $q_h = -q_c = +30$ K/ns. Upon cooling, $e(T)$ departs from the equilibrium liquid curve $e_{eq}(T)$ at high T . On reheating, the $e(T)$ curve overshoots the $e_{eq}(T)$ curve. This agrees with experiments [as indicated schematically in Fig. 1(a)]. Furthermore, Fig. 2(c) shows that $e(T)$ upon cooling at $q_c = -30$ K/ns and heating at $q_h = -q_c = 30$ K/ns coincides with $e_{eq}(T)$ for approximately $T > 230$ K. This is because, for $T > 230$ K, the relaxation time of the system becomes comparable to the cooling-heating time scale given by $1 \text{ K}/q_h = 1 \text{ K}/|q_c|$ and the system always has time to reach equilibrium before T changes considerably.

Figure 3 shows the effects of q_c on $C_V(T)$ upon heating the glass. We show $C_V(T)$ when heating two different glasses: the “slow-quenched glass” (SQG) obtained with a small cooling rate $q_c = -30$ K/ns and the “fast-quenched glass” (FQG) obtained with a much larger cooling rate $q_c = -10^4$ K/ns. DSC upscannings from SQG and FQG have been recently studied [16,37,38]. A characteristic feature during slow upscannings of FQG is the development of a valley in $C_V(T)$ for $T < T_g$ (see, e.g., [39]). The presence of this valley is related to the structural relaxation which manifests itself in the exploration of deeper and deeper basins in the potential energy landscape [9]. Results shown in Fig. 3 are very similar to those found for soda-lime-silicate glass fibers [37], basalt glasses [39], and propylene glycol [40].

Annealing below T_g is crucial in determining the glass transition temperature from DSC experiments, particularly for FQG. Annealing the FQG before upscanning can modify the shape of the valley in $C_V(T)$ upon heating [39] or it can produce a prepeak in $C_V(T)$ before the glass transition [11]. We age our FQG at $T_{age} = 180$ K for different times $0 < t_{age} \leq 20$ ns (see Fig. 4). Results obtained for $T_{age} = 100$ K have

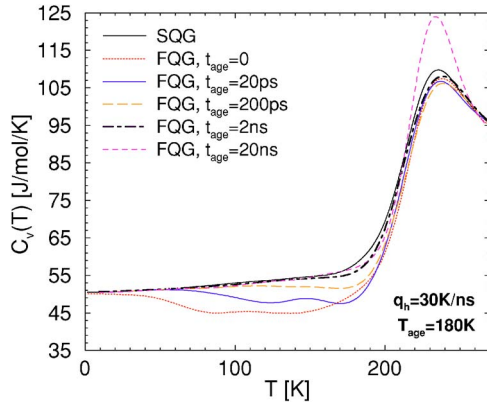


FIG. 4. (Color online) Specific heat upon heating the fast-quenched glass (FQG) after aging at $T_{\text{age}} = 180$ K for different aging times t_{age} . As t_{age} increases, the valley in $C_V(T)$ disappears and values of $C_V(T)$ approach the corresponding values obtained upon heating the slow-quenched glass (SQG).

been reported in Ref. [17]. At both $T_{\text{age}} = 100$ K and $T_{\text{age}} = 180$ K, we see that aging reduces the valley in $C_V(T)$ and that, as t_{age} increases, the curve of $C_V(T)$ evolves to the curve obtained for the SQG in Fig. 3. As expected, a comparison of $C_V(T)$ in Fig. 4 and in Fig. 2(a) of Ref. [17] shows that the relaxation at $T_{\text{age}} = 180$ K is much faster than it is at $T_{\text{age}} = 100$ K. After aging for $t_{\text{age}} = 20$ ns at $T_{\text{age}} = 100$ K we still find a valley in $C_V(T)$ while it already disappears at $T_{\text{age}} = 180$ K. It is interesting to note that Fig. 4 shows no sign of the “shadow glass transition” at $T_{\text{age}} = 180$ K [i.e., there is no prepeak in $C_V(T)$ for $T < T_g$] that is found at $T_{\text{age}} = 100$ K [17]. However, as t_{age} increases we observe the formation of a small and smooth maximum at $t_{\text{age}} = 20$ ps *within* the valley at $T \approx 150$ K. This smooth maximum seems to move to higher T for $t_{\text{age}} = 2$ ns and finally appears as a peak superposed on the “glass-transition peak” at $T \approx 250$ K. Some of the features observed in Fig. 4 are also observed in experiments. For example, it is reported in Ref. [11] that measurements of specific heat after aging samples of PVC at $T_{\text{age}} = 60$ °C show the presence of a prepeak below T_g . Moreover, this prepeak moves to higher T as t_{age} increases and finally overlaps the “glass-transition peak” for long t_{age} [39].

B. Narayanaswamy-Moynihan and Adam-Gibbs-Scherer expressions for the relaxation time

In this section, we compare the TNM approach predictions with our simulations using both the NM and AGS expressions. Figure 5 shows $C_V(T)$ obtained upon heating the SQG in the $(-30/+30)$ run. We also show the corresponding predictions of the TNM approach using both the NM and AGS expressions. Both the NM and AGS expressions give satisfactory results. The parameters are given in Table I.

The TNM approach with the AGS and NM expressions provides approximate expressions to calculate the q_c dependence of T'_f , defined as the fictive temperature in the glass state [see Fig. 1(a)]. Scherer [22] analyzed the experimental data and the TNM approach with the AGS expression to show that for $T = T'_f$,

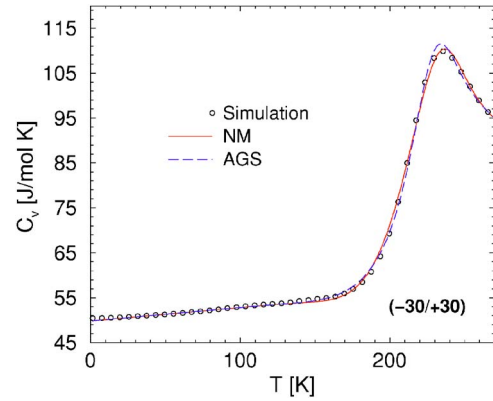


FIG. 5. (Color online) Specific heat upon heating the SQG at $q_h = -q_c = +30$ K/ns. We show the results from simulations and the predictions of the TNM approach using both the Narayanaswamy-Moynihan (NM) and the Adam-Gibbs-Scherer (AGS) expressions for the relaxation time. Both expressions predict the correct behavior of $C_V(T)$. The corresponding fitting parameters are reported in Table I.

$$\ln|q_c| \sim \ln \tau(T = T'_f) \sim -\frac{E_A}{T'_f S_c(T'_f)}. \quad (16)$$

An equivalent expression has been presented by Moynihan *et al.* [41,42] for the TNM approach with the NM expression

$$\ln|q_c| \sim \ln \tau(T = T'_f) \sim -\frac{\Delta h^*}{RT'_f}. \quad (17)$$

Scherer also found [22] that for small $|q_c|$, both expressions give similar results but that the AGS is better for large $|q_c|$ (i.e., for relaxation far from equilibrium). A quantitative relationship between the AGS and NM parameters can be obtained (see, e.g., Ref. [24]).

We evaluate $T'_f(q_c)$ to test the consistency of the fitting parameters found upon heating in the $(-30/+30)$ run. Figure 6 shows $T'_f(q_c)$ from MD simulations and the prediction of Eq. (16) for the AGS expression (dotted line) [43]. We use $E_A = 27626$ J/mol—i.e., the value obtained with the TNM approach for the $(-30/+30)T$ trajectory. The agreement between the data from our simulations for $T'_f(q_c)$ and the prediction in Eq. (16) is very good and shows that the parameters found with the AGS expression are consistent with the TNM approach.

The inset of Fig. 6 shows the results from MD simulations and the predictions of Eq. (17) for the NM expression. Equation (17) can be approximately satisfied only when reducing the range of the $|q_c|$ values by eliminating the point corresponding to $|q_c| = 10^5$ K/ns. The resulting fit shown in the inset of Fig. 6 suggests that $\Delta h^*/R = 12155$ K for $|q_c| \leq 10^4$ K/ns while consistency with the TNM fitting parameters obtained from the $(-30/+30)$ run (see Table I) requires $\Delta h^*/R = 4632$ K. The disagreement is considerable, suggesting that the parameters found with the NM expression are inconsistent with the TNM prediction.

Because the NM expression fails to describe the behavior of $T'_f(q_c)$ [Eq. (17)] and since the AGS expression requires

TABLE I. Best fitting parameters obtained for the TNM approach with the NM expression (top) and the AGS expression (bottom) for the relaxation time. In both cases, the values of the parameters agree with typical values obtained in experiments (e.g., see [5,24]). The error function ψ , defined in Eq. (15), is also indicated.

$(q_c/q_h)[\text{K/ns}]$	$-\ln(A/ns)$	β	x	$\Delta h^*/R [\text{K}]$	ψ
(-30/+30)	22.36	0.525	0.635	4632	0.017
(-10 ⁴ /+30)	52.79	0.734	0.083	11465	0.848
$(q_c/q_h)[\text{K/ns}]$	$-\ln(A/ns)$	β	$E_A[\text{J/mol}]$	ψ	
(-30/+30)	9.86	0.519	27626	0.010	
(-10 ⁴ /+30)	11.35	0.437	26550	2.325	

only three fitting parameters (instead of four for the NM expression), we conclude that the AGS expression is better suited to describe our results from simulations. Furthermore, the AGS also has the advantage of the source of nonlinear behavior below T_g being identified with the quantity $S_c(T)$ measured at equilibrium.

C. Fast-quenched glasses and the TNM approach

Figure 7 shows the predictions of the TNM approach while heating the FQG in the (-10⁴/+30) run. The parameters are those corresponding to the best fit of $e(T)$ upon heating in the (-30/+30) run. Clearly, Fig. 7 shows that both

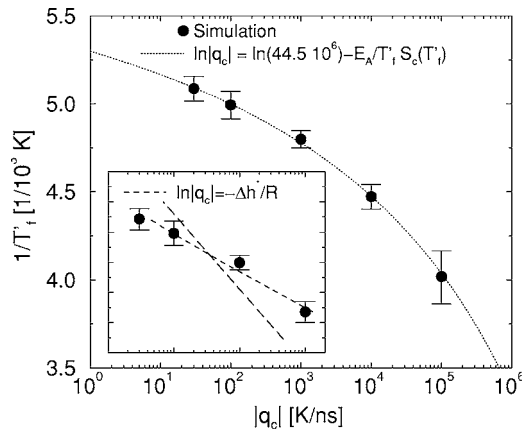


FIG. 6. Fictive temperature of the glass $T_f'(q_c)$ [43] [defined schematically in Fig. 1(a)] after cooling the liquid at different cooling rates q_c . The dotted line is the functional proposed by Scherer [Eq. (16)] using the AGS expression. In Eq. (16) we use $E_A = 27\,626 \text{ J/mol}$ —i.e., the value that gives the best fit of $e(T)$ with the TNM approach in the (-30/+30) run. The data from simulations fully agree with the prediction of Scherer for $T_f'(q_c)$. Inset: the TNM approach with the NM expression predicts a linear relation between $1/T_f'$ and $\ln|q_c|$. The dashed line is the interpolation of the data from simulation, where we eliminate the point for $|q_c| = 10^5 \text{ K/ns}$ (see text). The long-dashed line is the expected relationship between $1/T_f'$ and $\ln|q_c|$ [Eq. (17)] predicted by the TNM approach with the NM expression [the fitting parameters are those from the (-30/+30) run given in Table I]. Results obtained with the NM expression are inconsistent with the relationship between $1/T_f'$ and $|q_c|$ as predicted by the TNM approach [Eq. (16)].

the NM and AGS expressions give unsatisfactory results for $e(T)$ and $C_V(T)$.

We apply the TNM approach to the (-10⁴/+30) run and find the best fitting parameters to be those that describe the result from simulations upon heating. The fitting parameters are reported in Table I. From Table I we note that the best fitting parameters (using both the NM and AGS expressions) corresponding to the (-10⁴/+30) run differ considerably from those corresponding to the (-30/+30) run. These differences are sharper for the NM expression. In Fig. 8 we compare the predictions of the TNM approach using the parameters from the (-10⁴/+30) run with the results from simulations. The TNM predictions for $e(T)$ improve considerably. However, the TNM predictions for $C_V(T)$ are still off. This suggests that the TNM approach either with the NM or AGS expression fails to predict the behavior of $C_V(T)$ during the upscannings of FQG. Experiments show the same inability of the TNM approach to describe relaxation involving FQG [5,23,37,44]; i.e., the TNM approach is not able to reproduce results in slow heatings of FQG across T_g .

Next we show that the deficiency of the TNM approach in describing the relaxation of FQG builds up during the prepa-

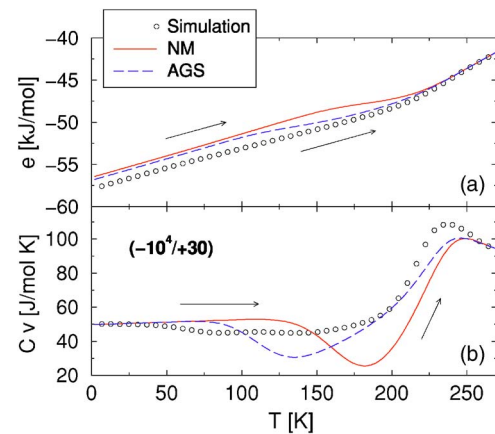


FIG. 7. (Color online) Heating of the FQG predicted by the TNM approach using both the NM [Eq. (12)] and the AGS [Eq. (13)] expressions for the relaxation time. The same fitting parameters as in Fig. 5 are used—i.e., those obtained from the best fitting of $e(T)$ using the TNM approach in the (-30/+30) run (see Table I). The disagreement between the TNM approach and the simulation is evident.

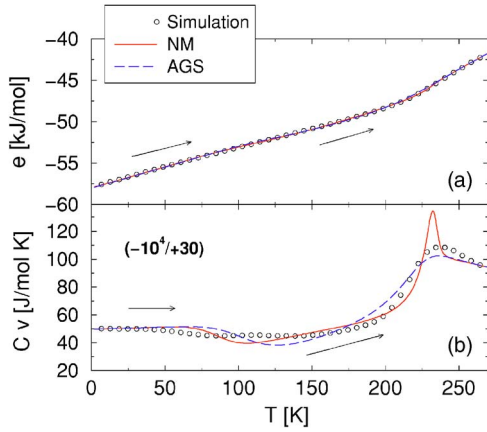


FIG. 8. (Color online) Comparison of the simulation results for (a) the energy and (b) the specific heat upon heating the FQG with the best fit prediction of the TNM approach (with both the NM and AGS expressions). Fitting parameters are reported in Table I. The $e(T)$ predictions of the TNM approach improve considerably with respect to Fig. 7. However, there is still a noticeable disagreement in $C_V(T)$.

ration of the glass—i.e., during the cooling process of the liquid. To do so, we investigate the predictions of the TNM approach for $e(T)$ when cooling the liquid at different rates q_c . The fitting parameters are those obtained from the $(-30/+30)$ run (see Table I). In Fig. 9, we compare the results from simulations with the predictions of the TNM approach using the AGS expression (we obtain similar results using the NM expression). As expected, the TNM approach gives a good prediction for $q_c = -30$ K/ns. However, as $|q_c|$ increases, the predicted values of $e(T)$ are higher than the corresponding values obtained from simulations. The devia-

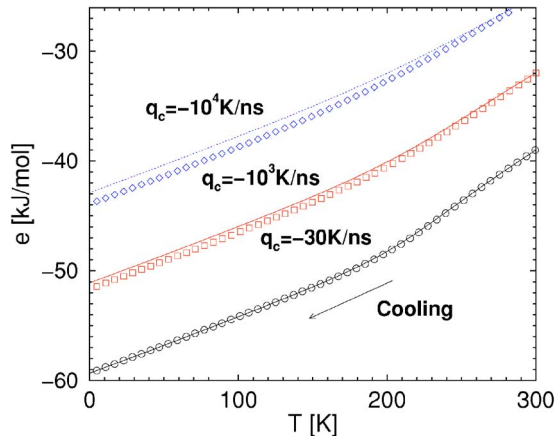


FIG. 9. (Color online) Temperature dependence of the energy upon cooling the liquid toward the glass state at different cooling rates q_c . Symbols are the simulations results while lines are predictions of the TNM approach using the AGS expression. Note that curves for $q_c = -10^3$ K/ns and $q_c = -10^4$ K/ns have been shifted for clarity by 7 kJ/mol and 14 kJ/mol, respectively. The same fitting parameters used in Fig. 5 to fit the curves have been used. Predictions of the TNM approach and simulations agree for $q_c = -30$ K/ns. However, deviations occur for $|q_c| > 30$ K/ns. The discrepancies become larger as $|q_c|$ increases.

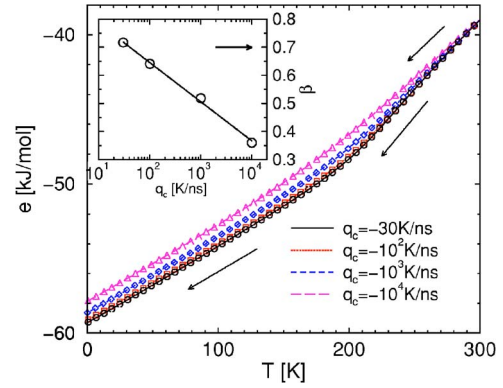


FIG. 10. (Color online) Prediction of the T dependence of the energy upon cooling the liquid toward the glass at different cooling rates q_c . Symbols refer to simulation data and lines correspond to the predictions of the TNM approach using the AGS. The fitting parameters are assumed to depend on q_c and are fitted independently (see Table II). The only parameter that shows a strong dependence on q_c is the stretching exponent β (see inset). Note that for the fastest cooling rate $\beta = 0.716$, which is close to the equilibrium value $\beta \approx 0.7$ (see arrow in inset) obtained in equilibrium simulations from the density correlation function for small wave vector. For slower cooling rates, $\beta \sim \ln|q_c|$.

tions are larger for increasing values of $|q_c|$. This means that both the NM and AGS expressions overestimate the value of $\tau(T, T_f)$ when using the parameters obtained from the $(-30/+30)$ run; i.e., the TNM approach predicts that the system relaxes to equilibrium much slower than it does.

D. Attempts to extend the TNM approach to fast-quenched glasses

1. Fitting parameters depending on q_c and q_h

Next, we discuss possible modifications for improving the TNM approach in order to describe the structural relaxation upon heating the FQG. In Fig. 9 we show that there are discrepancies between the predictions of the TNM approach and simulations and that the differences increase as $|q_c|$ increases. This suggests that the fitting parameters might depend on the cooling and/or heating rate. Therefore, one could assume that the fitting parameters depend (i) on only the cooling rate or (ii) on both the cooling and heating rates. To explore these ideas we will restrict the discussion to the AGS expression because, as we find in Sec. IV B (see also Fig. 6), the NM expression is not well suited for describing our results from simulations.

(i) Figure 10 shows the best fit of $e(T)$ when applying the TNM approach. The TNM predictions fully agree with the results from simulations. We find that allowing only β and A to depend on q_c is sufficient for good results upon cooling; i.e., there is no need to assume that $E_A = E_A(q_c)$. The fitting parameters are given in Table II. We observe that $\ln(A) \approx \text{const}$ while β shows a clear logarithmic dependence on q_c (see the inset of Fig. 10).

We note that for the fastest cooling rate we obtain $\beta = 0.716$, which is close to the value $\beta \approx 0.7$, obtained in equi-

TABLE II. Best fitting parameters obtained with the TNM approach using the AGS expressions for the relaxation time. $E_A = 27\,626$ J/mol, the other fixed value, is obtained from the $(-30/+30)$ run. In this way, Eq. (16) is satisfied (see also Fig. 6).

q_c [K/ns]	$-\ln(A/ns)$	β
-30	10.33	0.716
-10^2	10.67	0.64
-10^3	11.09	0.517
-10^4	11.16	0.359

librium simulations from the density correlation function for small wave vectors [45]. The stretching exponent β is usually interpreted as a measure of the width of the distribution of relaxation times. This suggests that after cooling at our largest cooling rate, the system “remembers” the starting configuration and the distribution of relaxation times does not change. For slower cooling rates, β decreases as $\beta \sim \ln|q_c|$, indicating that the structural relaxation occurring upon cooling changes the distribution of relaxation times.

Next, we test the TNM approach with $e(T)$ obtained upon heating in the $(-10^4/+30)$ run. We use the parameters obtained for $q_c = -10^4$ K/ns in Table II. The results can be observed in Fig. 11 and are not as good as those shown in Fig. 5.

(ii) We also test the TNM approach by assuming that the fitting parameters depend on both the cooling and heating rates. In this case, we use the parameters for $q_c = -10^4$ K/ns given in Table II during the cooling part of the $(-10^4/+30)$ run and those obtained for the $(-30/+30)$ run, given in Table I, during the heating part of the $(-10^4/+30)$

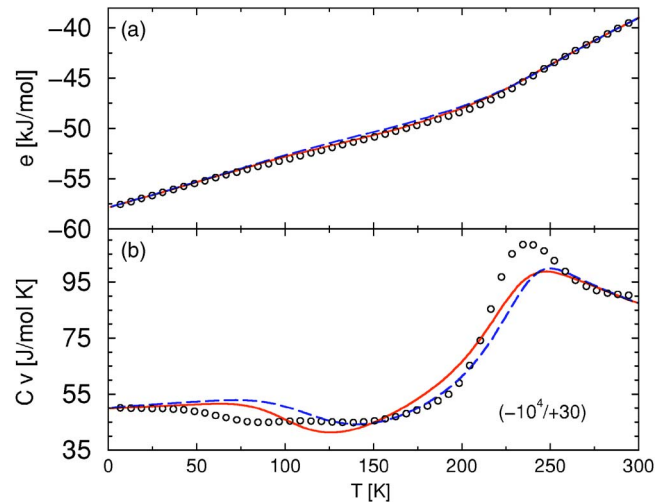


FIG. 11. (Color online) (a) Energy and (b) specific heat upon heating the FQG. The symbols correspond to simulation data. The solid line is the prediction of the TNM approach with the AGS expression using the same parameters as in Fig. 10 for the case $q_c = -10^4$ K/ns (Table II). The long-dashed line corresponds to the TNM prediction using the fitting parameters of the cooling run at $q_c = -10^4$ K/ns upon cooling and the fitting parameters of the $(-30/+30)$ run (Table I) upon heating. In both cases, the results are unsatisfactory.

run. The results are unsatisfactory, as we can see in Fig. 11. Therefore, these results suggests that the TNM approach cannot be improved by assuming a cooling-heating rate dependence of the fitting parameters.

2. Fitting parameters depending on T or T_f

Another plausible modification to the TNM approach is to assume that the fitting parameters depend on T and/or T_f . In fact, due to the good results obtained during cooling with $E_A = \text{const}$ we will assume that E_A does not depend on T and/or T_f . Moreover, since $\ln(A)$ shows a very weak dependence on q_c for different cooling trajectories (see Table II), we also assume that $\ln(A)$ does not depend on T or T_f . This implies that the only modification to the AGS expression we can make is to allow $\beta = \beta(T, T_f(T))$. Assuming that $\beta = \beta(T, T_f(T))$ or just $\beta = \beta(T)$ means that we are rejecting the “thermorheological simplicity” hypothesis; i.e., we are assuming that the spectrum of relaxation times [23] changes during the structural relaxation. We note that Lubchenko and Wolynes (LW) [46] recently extended the random first-order transition theory of supercooled liquids to treat aging phenomena in nonequilibrium structural glasses. LW found that the stretching exponent should be a function of T and T_f —i.e., $\beta = \beta(T, T_f(T))$. Due to the good fitting of $e(T)$ obtained with the TNM approach upon cooling at $q_c = -10^4$ K/ns using $\beta = 0.359$, we will assume that β depends appreciably on T only upon heating and that the initial value before heating is $\beta = 0.359$. In summary, we assume that $E_A = 27\,626$ J/mol, $\ln(A/ns) = -11.36$, and $\beta = 0.359$ during the cooling part of the trajectory and $\beta = \beta(T)$ during the heating part [47].

Figure 12 shows (a) $e(T)$ and (b) $C_V(T)$ obtained with the best fitting of $\beta = \beta(T)$ to $e(T)$ in the $(-10^4/+30)$ run. The prediction of the TNM approach for $e(T)$ agrees with simulations only up to $T \approx 140$ K. The effect of these deviations in $e(T)$ is very strong in $C_V(T)$. Evidently, assuming that $\beta = \beta(T)$ does not solve the problems of the TNM approach for heatings of the FQG.

Figure 13 shows (a) $\beta(T)$, (b) $\tau(T)$ [from Eq. (13)], and (c) $T_f(T)$ [from Eq. (11)]. For $T < 60$ K we find that $\beta(T) \approx \text{const}$ and $\tau(T) > 1$ s, which implies that the system is practically unable to relax for simulation time scales. This is confirmed in Fig. 13(c), where we see that $T_f(T) \approx \text{const}$ for $T < 50$ K.

The AGS expression is acceptable up to $T \approx 140$ K [where the prediction of the TNM approach for $e(T)$ agrees with simulations], and we find that β is only weakly T dependent. Beyond $T \approx 140$ K, $\beta(T)$ decreases abruptly. Equation (5) implies that the lower the value of β is, the slower the relaxation is. This suggests that the AGS expression at $T > 140$ K gives smaller values of τ than those required by the TNM approach if β was a constant. At $T \approx 165$ K we find that $\beta(T) = 0$. Indeed, the TNM approach with $\beta = 0$ implies that the response function [see Eq. (5)] is independent of τ , which has no physical sense. Furthermore, it is also assumed in the KWW expression that $0 < \beta \leq 1$. This is probably why the TNM approach fails above $T \approx 140$ K and why β shows a strange behavior going from negative values to values

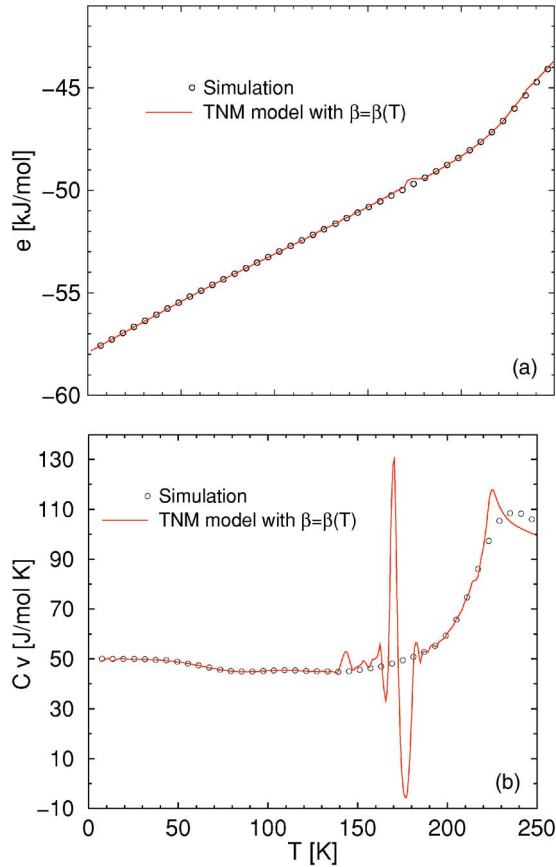


FIG. 12. (Color online) Temperature dependence of (a) the energy and (b) the specific heat upon heating the FQG. The lines are the predictions resulting from the TNM approach using the AGS expression and assuming that the parameter β changes with T [parameters E_A and $\ln(A)$ are fixed to the values reported in Table II for $q_c = -10^4$ K/ns]. The TNM approach gives reasonable results up to $T \approx 140$ K, but deviations occur at higher temperatures.

larger than 1. This is probably also the cause of the oscillations in $C_V(T)$ observed in Fig. 12(b).

E. Aging the glass and the TNM approach

We study two other thermal histories and test the TNM approach while aging the fast-quenched glass at $T_{\text{age}} = 100$ K and $T_{\text{age}} = 180$ K—i.e., above and below $T = 140$ K—which is the T at which the TNM approach starts to fail for the $(-10^4/+30)$ run. We repeat the procedure mentioned above and assume that $\beta = \beta(t_{\text{age}})$ [instead of $\beta = \beta(T)$] [48]. Figure 14(a) shows the evolution of $e(t_{\text{age}})$ while the fast-quenched glass is aged at $T_{\text{age}} = 100$ K. We also show the predictions of the TNM approach with the AGS expression assuming that $E_A = 27\,626$ kJ/mol and $\ln(A/\text{ns}) = -11.36$ —i.e., the values found upon cooling the liquid at $q_c = -10^4$ K/ns (see Table II). We show the case for $\beta = 0.359$ (the value obtained upon cooling at $q_c = -10^4$ K/ns) and the case for $\beta = \beta(t_{\text{age}})$. Clearly, the results with $\beta = 0.359$ are unacceptable while when $\beta = \beta(t_{\text{age}})$ the TNM approach provides a good fit of the numerical data at $T_{\text{age}} = 100$ K. This can be expected since $T_{\text{age}} < 140$ K. The be-

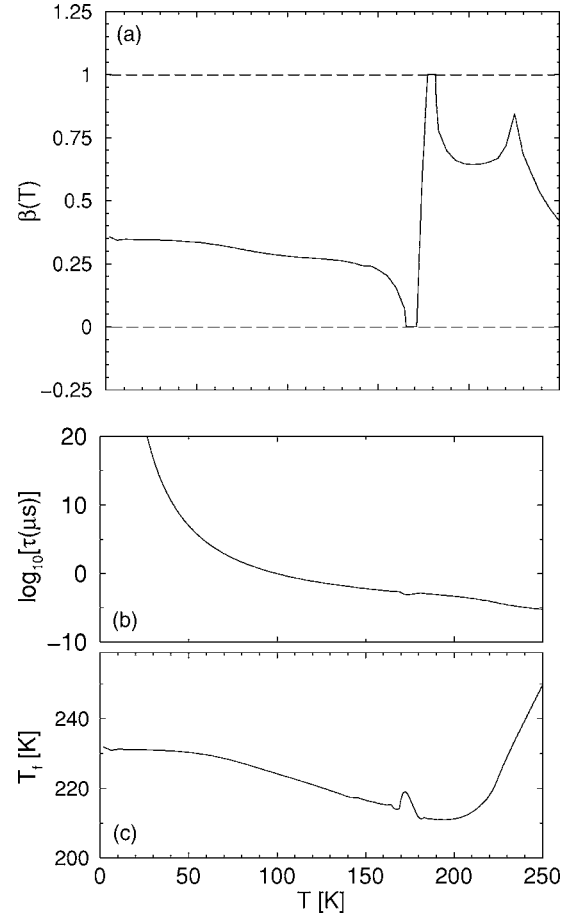


FIG. 13. Temperature dependence of (a) the parameter $\beta(T)$ used in Fig. 12, (b) the relaxation time τ predicted from the AGS expression [Eq. (13)], and (c) the fictive temperature T_f [Eq. (11)]. Data above $T = 160$ K [when $\beta(T) = 0$] have no physical meaning.

haviors of $\beta(t_{\text{age}})$, $\tau(t_{\text{age}})$, and $T_f(t_{\text{age}})$ are shown in Fig. 14(b).

As t_{age} increases, we find that $\beta(t_{\text{age}})$ decreases suggesting that the AGS expression gives smaller values of τ than those required by the TNM approach if $\beta(t_{\text{age}}) = 0.359$. This behavior of $\beta(t_{\text{age}})$ is consistent with the discussion in Sec. IV D 2, where the importance of the T dependence of β is discussed. Figure 14(b) shows that $\tau(t_{\text{age}})$ increases with t_{age} . This behavior of $\tau(t_{\text{age}})$ might seem counterintuitive because τ is usually an increasing function of T and, in our case, T increases from ≈ 0 K to 100 K at $t_{\text{age}} = 0$. The solution to this puzzle is provided in Fig. 14(c) where we show $T_f(t_{\text{age}})$. We see that $T_f(t_{\text{age}} = 0) = 230$ K $>$ T_{age} . This means that the system during aging is relaxing from a typical structure corresponding to $T = 230$ K toward one corresponding to a lower T . Therefore, τ also evolves from $\tau(T \approx 230$ K) to $\tau(T < 230$ K), meaning that it must increase during aging.

We show the results for $T_{\text{age}} = 180$ K in Fig. 15. For comparison, we also show the case in which $\beta = \text{const} = 0.359$. The results in both cases are unsatisfactory. However, we note that Fig. 15(a) suggests that the TNM approach could possibly predict the MD results in the asymptotic limit of t_{age} . We cannot formulate any conclusion on this point because longer simulations would be needed.

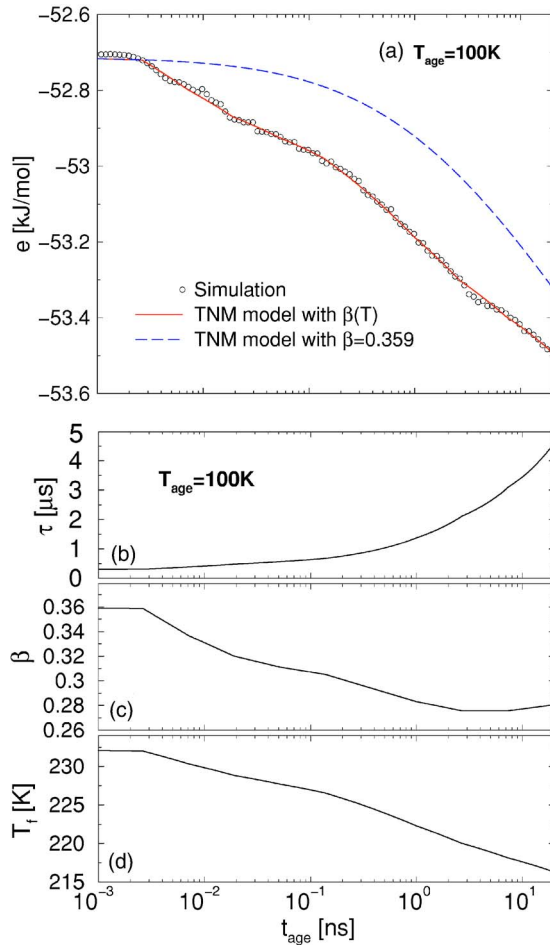


FIG. 14. (Color online) (a) Aging time dependence of the energy during aging the FQG at temperature $T_{\text{age}} = 100$ K. The long-dashed line is the prediction of the TNM approach using the AGS expression with the parameters obtained from the cooling run at $q_c = -10^4$ K/ns (Table II). The solid line is the prediction of the TNM approach when $\beta = \beta(t_{\text{age}})$. At $T_{\text{age}} = 100$ K, the TNM approach succeeds by $\beta = \beta(t_{\text{age}})$. The corresponding aging time dependences of the predicted (b) relaxation time τ , (c) fitted $\beta(t_{\text{age}})$, and (d) predicted fictive temperature for $\beta = \beta(t_{\text{age}})$ are also shown.

Similar to the case for $T_{\text{age}} = 100$ K [Fig. 14(d)], at $T_{\text{age}} = 180$ K [Fig. 15(d)] we observe a monotonic decay of T_f , indicating that the system is still relaxing to T_{age} from $T > T_{\text{age}}$. The relaxation is faster at $T_{\text{age}} = 180$ K, so the system reaches lower T_f than at $T_{\text{age}} = 100$ K. This means that, for a given T_{age} , $\tau(t_{\text{age}})$ reaches a larger value at $T_{\text{age}} = 180$ K than at $T_{\text{age}} = 100$ K. The behavior of $\beta(t_{\text{age}})$ in Fig. 15(b) is reminiscent of Fig. 13(a) where upon heating the fast-quenched glass, $\beta = \beta(T)$.

V. DISCUSSION

Presently available computational facilities allow us to follow the dynamics of a model system over approximately eight orders of magnitude of time or, equivalently, for approximately 10^8 integration time steps, offering the possibility of studying how the cooling rate affects the formation of

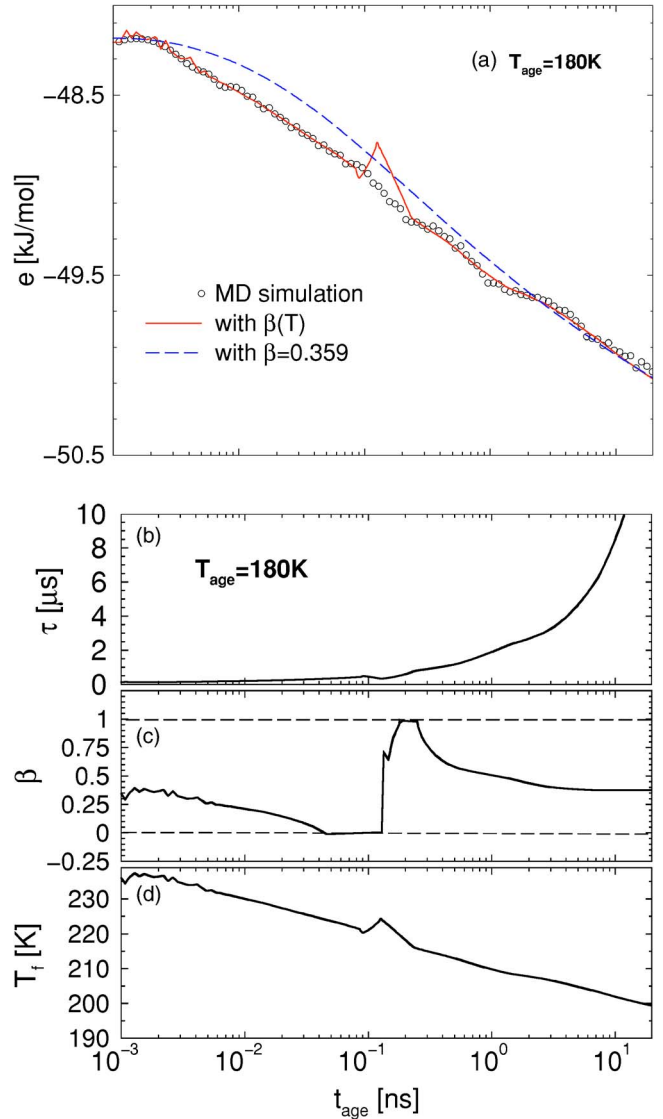


FIG. 15. (Color online) Same as in Fig. 14, but with $T_{\text{age}} = 180$ K.

disordered arrested glass structures. Simulations allow us to generate glasses with cooling rates differing by as much as a factor of approximately 10^4 . While the absolute rates in simulations and experiments differ by several orders of magnitude, simulations are able to reproduce the cooling-heating rate dependence of the DSC experimental phenomenology.

In this paper we have described the simulated cooling and heating DSC runs we have carried out using the SPC/E model of water. We have shown that the T dependence of the specific heat during cooling and heating runs, as well as the cooling rate effects, can indeed be properly reproduced. The agreement between the simulations and the experimental data suggests that a detailed comparison of the numerical data with the phenomenological TNM approach, the method commonly used in the interpretation of the DSC measurements, is possible. We have tested two different propositions for the T and T_f dependence of the relaxation time: the NM [Eq. (17)] and the AGS [Eq. (16)] expressions. We find that for slow-cooled glasses the TNM-AGS approach provides a

consistent description of the numerical data. For fast-cooled glasses, neither the TNM-AGS nor TNM-NM approach is able to provide a description of the T dependence of the specific heat. We have extended the TNM approach by assuming that the fitting parameters can depend on T and/or q . For cooling runs, a q dependence of the stretching exponent β results in an agreement between the TNM approach and numerical data. However, we did not find any significant improvement when fitting the cooling and heating runs.

Among the possible reasons for the failure of the TNM approach are the use of [49] (i) the AGS or NM expression for the relaxation time $\tau(T, T_f)$, (ii) the expression of the response function $\phi(t', t)$, as given by the KWW expression [Eq. (4)], and (iii) the superposition principle, by which the evolution of $T_f(T)$ is expressed as the sum of the differential perturbations $\Delta T'$ occurred each at T' [see Eq. (7)].

Hypothesis (iii) is the weakest. Indeed, when we fit data from the $(-30/+30)$ trajectory, we find that the TNM ap-

proach works. In this case, $T - T_f(T)$ is small. However, when fitting data from the $(-10^4/+30)$ run, $T - T_f(T)$ can be as large as 130 K [e.g., see Fig. 13(c)]. Therefore it seems that only when $T - T_f(T)$ is small, and hence only when the linear superposition principle is satisfied, does the TNM provide a detailed description of the DSC data.

Our work suggests that present-day simulation techniques can be successfully used to test the individual hypotheses implicit in the TNM approach. Hence, simulations could, and should, be used to improve the TNM approach. We hope that results from future studies will provide a guide for a more accurate modeling of DSC data.

ACKNOWLEDGMENTS

We thank I.M. Hodge for enlightening comments of the manuscript. We thank NSF Chemistry Grant Nos. CHE0096892 and CHE0404673 and MIUR Firb.

-
- [1] P. G. Debenedetti, *Metastable Liquids* (Princeton University Press, Princeton, 1996).
- [2] W. Kauzmann, *Chem. Rev.* (Washington, D.C.) **43**, 219 (1948).
- [3] C. A. Angell, *Science* **267**, 1924 (1995).
- [4] G. W. Scherer, *Relaxation in Glass and Composites* (Wiley, New York, 1986).
- [5] I. M. Hodge, *J. Non-Cryst. Solids* **169**, 211 (1994).
- [6] I. M. Hodge and A. R. Berens, *Macromolecules* **14**, 1598 (1981).
- [7] I. M. Hodge and A. R. Berens, *Macromolecules* **15**, 762 (1981).
- [8] W. Kob, F. Sciortino, and P. Tartaglia, *Europhys. Lett.* **49**, 590 (2000).
- [9] N. Giovambattista, H. E. Stanley, and F. Sciortino, *Phys. Rev. E* **69**, 050201 (2004).
- [10] C. T. Moynihan *et al.*, *Ann. N.Y. Acad. Sci.* **279**, 15 (1976).
- [11] A. R. Berens and I. M. Hodge, *Macromolecules* **756**, 15 (1982).
- [12] A. J. Kovacs, J. J. Aklonis, J. M. Hutchinson, and A. R. Ramos, *J. Polym. Sci., Polym. Phys. Ed.* **17**, 1097 (1979); A. J. Kovacs, *Fortschr. Hochpolym.-Forsch.* **3**, 394 (1963).
- [13] H. Sasabe and C. T. Moynihan, *J. Polym. Sci., Polym. Phys. Ed.* **16**, 1447 (1978).
- [14] I. M. Hodge and G. S. Huvard, *Macromolecules* **16**, 371 (1983).
- [15] M. A. DeBolt, A. J. Easteal, P. B. Macedo, and C. T. Moynihan, *J. Am. Ceram. Soc.* **59**, 16 (1976).
- [16] Y. Z. Yue and C. A. Angell, *Nature (London)* **427**, 717 (2004).
- [17] N. Giovambattista, C. A. Angell, F. Sciortino, and H. E. Stanley, *Phys. Rev. Lett.* **93**, 047801 (2004).
- [18] G. W. Scherer, *J. Non-Cryst. Solids* **123**, 75 (1990).
- [19] A. Q. Tool, *J. Am. Ceram. Soc.* **29**, 240 (1946).
- [20] R. Gardon and O. S. Narayanaswamy, *J. Am. Ceram. Soc.* **53**, 380 (1970); O. S. Narayanaswamy, *ibid.* **54**, 491 (1971).
- [21] G. Adam and J. H. Gibbs, *J. Chem. Phys.* **43**, 139 (1965).
- [22] G. W. Scherer, *J. Am. Ceram. Soc.* **67**, 504 (1984).
- [23] G. W. Scherer, *J. Am. Ceram. Soc.* **69**, 374 (1986).
- [24] I. M. Hodge, *Macromolecules* **20**, 2897 (1987); *J. Non-Cryst. Solids* **131-133**, 435 (1991).
- [25] I. M. Hodge, *Macromolecules* **16**, 898 (1983).
- [26] H. J. C. Berendsen, J. R. Grigera, and T. P. Stroatsma, *J. Phys. Chem.* **91**, 6269 (1987).
- [27] H. J. C. Berendsen *et al.*, *J. Chem. Phys.* **81**, 3684 (1984).
- [28] In Eq. (1), T_f is defined based on $e(T)$ and should be written $T_{f,e}$ because T_f can also be defined in terms of any other macroscopic property (e.g., enthalpy, volume, refraction index, etc.). Furthermore, $T_f(T)$ defined from different properties are not necessarily equal. In this work we will use the fictive temperature obtained from $e(T)$ and identify it as $T_f(T)$.
- [29] M. D. Ediger, C. A. Angell, and S. R. Nagel, *J. Phys. Chem.* **100**, 13200 (1996).
- [30] F. Sciortino, E. La Nave, and P. Tartaglia, *Phys. Rev. Lett.* **91**, 155701 (2003).
- [31] A. Scala, F. W. Starr, E. La Nave, F. Sciortino and H. E. Stanley, *Nature (London)* **406**, 166 (2000).
- [32] S. Sastry, *Nature (London)* **409**, 164 (2001).
- [33] We find that this is a good approximation for $0 < T < 155$ K [see also Fig. 2(b)]. We obtain $a_0 = 0.037$ J/(mol K) and $b_0 = 6R$ (as expected from the equipartition theorem for a rigid molecule model). Similar approximations are commonly made in experiments—e.g., [10].
- [34] To obtain $e_{eq}(T)$, we fit $e_{eq}(T)$ [see also Fig. 2(a)] with a fourth-order polynomial, $e_{eq}(T) = A_0 + B_0T + C_0T^2 + D_0T^3$, for $T > 190$ K (we test that this range of T corresponds to the values taken by T_f upon cooling and heating). We find that $A_0 = -77.29$ kJ/mol, $B_0 = 0.1742$ kJ/mol/K, $C_0 = -1.76 \times 10^{-4}$ kJ/mol/K², and $D_0 = 6.9 \times 10^{-8}$ kJ/mol/K³.
- [35] We note that experimentalists prefer using Eq. (2) instead of Eq. (1) because in DSC studies the observable is the specific heat. We prefer to use Eq. (1) because in MD simulations, energy is the standard quantity measured. Furthermore, to use Eq. (2) we need to evaluate $C_V^{eq}(T_f)$ down to approximately 190 K. This is another problem for SPC/E because, as we will

see, $C_V^{cq}(T_f)$ strongly depends on temperature and from our MD data of $C_V(T)$ we can obtain $C_V^{cq}(T_f)$ only for $T_f > 210$ K. This means we need to extrapolate $C_V^{cq}(T_f)$ from ≈ 210 K down to $T \approx 190$ K. This extrapolation can produce large errors for $C_V^{cq}(T_f)$.

- [36] M. Oguni and C. A. Angell, J. Chem. Phys. **78**, 7334 (1983).
 [37] J. Huang, and P. K. Gupta, J. Non-Cryst. Solids **151**, 175 (1992).
 [38] V. Velikov, S. Borick, and C. A. Angell, Science **294**, 2335 (2001).
 [39] Y. Z. Yue, S. L. Jensen, and J. deC. Christiansen, Appl. Phys. Lett. **81**, 2983 (2002).
 [40] C. A. Angell, Y. Z. Yue, L. M. Wang, J. R. D. Copley, S. Borick, and S. Mossa, J. Phys.: Condens. Matter **15**, 51051 (2003).
 [41] C. T. Moynihan, A. J. Easteal, M. A. DeBolt, and J. Tucker, J. Am. Ceram. Soc. **59**, 12 (1976).
 [42] C. T. Moynihan, A. J. Easteal, J. Wilder, and J. Tucker, J. Phys. Chem. **78**, 2673 (1974).
 [43] To calculate $T_f'(q_c)$ we use the construction indicated in Fig. 1(a). We first obtain the straight line tangent to $e(T)$ for $0 \leq T \leq T^*$, where T^* is an arbitrary temperature. The intersection of this line with the curve $e_{cq}(T)$ defines T_f' . The error bars in Fig. 6 correspond to the different values of T_f' obtained by changing T^* between 0 K and 150 K.
 [44] C. T. Moynihan, S. N. Crichton, and S. M. Opalka, J. Non-Cryst. Solids **131-133**, 420 (1991).
 [45] F. Sciortino, L. Fabbian, S-H. Chen, and P. Tartaglia Phys. Rev. E **56**, 5397 (1997).
 [46] V. Lubchenko and P. G. Wolynes, J. Chem. Phys. **121**, 2852 (2004).
 [47] To calculate $\beta(T)$, we divide the T range upon heating into m intervals. The values of T and $\beta(T)$ at the beginning of each interval are given by T_i and β_i , respectively ($i=1,2,\dots,m$), and within each interval $[T_i, T_{i+1}]$ we assume that $\beta(T)$

is a linear function of T —i.e., for $T_i < T < T_{i+1}$, $\beta(T) = \beta_i + (T - T_i)(\beta_{i+1} - \beta_i)/(T_{i+1} - T_i)$. Therefore, in the present implementation of the TNM approach we follow the same method explained in Sec. III B. In Eq. (11) we only replace $\beta \rightarrow \beta_k$, where $\beta_k = \beta_i + (T_k - T_i)(\beta_{i+1} - \beta_i)/(T_{i+1} - T_i)$ for $i \leq k < i+1$.

- [48] Due to the slow dynamics below T_g , to fit $\beta(t_{age})$ we divide the t_{age} range into m intervals using a logarithmic time scale. The values of t_{age} and $\beta(t_{age})$ at the beginning of each interval are given by $t_{e,i}$ and β_i , respectively ($i=1,2,\dots,m$). Furthermore, we assume that at each interval $[t_{age,i}, t_{age,i+1}]$ the function $\beta(t_{age})$ is linear with $\ln(t_{age})$ —i.e., for $t_{age,i} < t_{age} < t_{age,i+1}$, $\beta(t_{age}) = \beta_i + [\ln(t_{age}) - \ln(t_{age,i})](\beta_{i+1} - \beta_i) / [\ln(t_{age,i+1}) - \ln(t_{age,i})]$. For the implementation of the TNM approach in the present case where $\beta = \beta(T_{age})$, we follow the method explained in Sec. III B. However, during aging dT_k/q_k must be replaced by $dT_k/q_k \rightarrow dt_k$ in Eq. (11), as proposed by Hodge and Berens [6,7]. Furthermore, our assumption that $\beta(t_{age}) = \beta_i + [\ln(t_{age}) - \ln(t_{age,i})](\beta_{i+1} - \beta_i) / [\ln(t_{age,i+1}) - \ln(t_{age,i})]$ implies that we must replace $\beta \rightarrow \beta_k = \beta_i + [\ln(t_{age,k}) - \ln(t_{age,i})](\beta_{i+1} - \beta_i) / [\ln(t_{age,i+1}) - \ln(t_{age,i})]$ in Eq. (11) during aging (here, $i \leq k < i+1$ and $m \leq n$).
 [49] In the present discussion we limit to the case where $C_v^{gl}(T)$ in Eq. (1) is independent of T_f . However, this is not necessarily the case. In fact, for approximately $T < 100$ K, $C_v^{gl}(T)$ depends only on the vibrational motion of the molecules (i.e., there is no structural relaxation at these T). In the potential energy landscape approach, this vibrational motion is determined by the shape of the basin around the IS characterizing the glass at T_f' . In Ref. [9], it is shown that the shape of the basins of the glass at $T \approx 0$ K is weakly dependent on q_c or, equivalently, on T_f' . Therefore, another possible reason for the failure of the TNM model to predict the structural relaxation in FQG is the assumption $C_v^{gl}(T, T_f) = C_v^{gl}(T)$ in Eq. (1).